The Gershberg-Papulis Method in the Problem of Phase Structure Reconstruction from Low-angle Hilbertograms

Eduard Arbuzov [1,2], Vitaly Arbuzov [1], Yuri Dubnishchev [1], Olga Zolotukhina [1], Michael Lapikov [1] and Vladimir Lukashov [1]

[1] *Kutateladze Institute of Thermophysics SB RAS, Novosibirsk, 630090, Russia*
[2] *Sobolev Institute of Mathematics SB RAS, Novosibirsk, 630090, Russia*

Abstract

The possibility of processing small-view hilbertograms by the Gershberg-Papulis method to restore the refractive index of phase objects is discussed. The method consists in iterative transitions from estimating a function in the Fourier plane to estimating it in a coordinate space with an adjustment using a priori information. The spectrum of the function is determined on the entire frequency plane as an iterative process result Numerical simulation of the refractive index reconstruction for various test functions was performed using the Gershberg-Papulis method using Radon data known for four angles. Experimental studies on the Hilbert diagnostics example of reacting media (flames) in a high-speed shooting mode (up to 2000 frames per second) were performed using a four-angle tomographic complex implemented on the basis of an upgraded IAB-463M shadow device.

Keywords

Hilbert optics, optical tomography, the Gershberg-Papoulis method.

1. Introduction

Hilbert optics is a powerful tool for analyzing light fields in optical systems [1]. Hilbert optics methods make it possible to restore phase functions more efficiently and accurately using information obtained from hilbertograms and to estimate, with appropriate processing, temperature fields and molar concentrations of combustion products [2, 3].

Computed tomography (CT) in optics is a method of reconstructing three-dimensional structures of objects based on their two-dimensional projections, which are formed using probing light fields [4, 5]. One of the key problems of optical CT is the problem associated with the difficulty of organizing a sufficient number of projections or a small angular range of diagnosing an object, which leads to loss of information or the impossibility of obtaining accurate values of the required parameters from processed tomograms.

The Gershberg-Papulis algorithm is one of the common methods for solving the problem of reconstructing the structures under study in low-angle tomography [6–8]. It is based on an iterative process that allows you to gradually refine the results, minimizing the discrepancies between experimental data and theoretical estimates at each iteration. As a result, a high quality of reconstruction can be achieved even with a limited number of projections.

The purpose of this work is to study the Gershberg-Papulis method and its application for the reconstruction of the phase optical density fields of gaseous, condensed and reacting (flames) media according to low-angle Hilbert tomography data.

GraphiCon 2023: 33rd International Conference on Computer Graphics and Vision, September 19-21, 2023
V.A. Trapeznikov Institute of Control Sciences of Russian Academy of Sciences, Moscow, Russia
EMAIL: arbuzov@math.nsc.ru (E. Arbuzov); arbuzov@itp.nsc.ru (V. Arbuzov); dubnistchev@itp.nsc.ru (Yu. Dubnishchev); melexina-olga17@ya.ru (O. Zolotukhina); mlapikov1@list.ru (M. Lapikov); luka@itp.nsc.ru (V. Lukashov)
ORCID: 0000-0001-9488-8650 (E. Arbuzov); 0000-0003-2404-526X (V. Arbuzov); 0000-0001-7874-039X (Yu. Dubnishchev); 0000-0003-3486-4459 (O. Zolotukhina); 0009-0009-0759-8627 (M. Lapikov); 0000-0001-8178-7607 (V. Lukashov)

2. Low-angle Hilbert tomography

The optical complex was developed to implement Hilbert tomography based on the upgraded shadow device [9] IAB-463M, which allows probing the object under study from four angles and synchronously recording tomographic projections of the visualized phase structures with one video camera (figure 1).

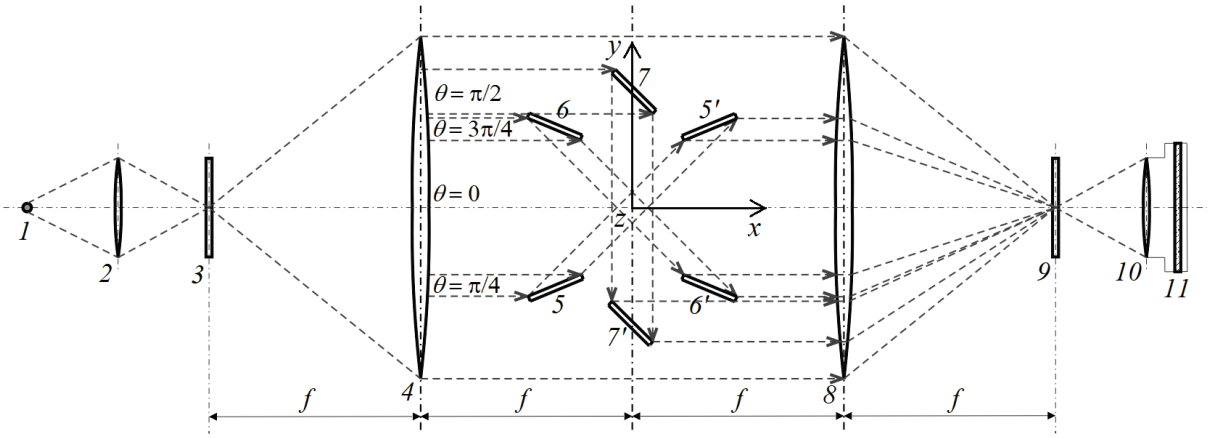

Figure 1: Simplified diagram of the Hilbert tomograph

The complex contains an illumination module consisting of a radiation source 1, the objective 2, and a slit diaphragm 3 placed in the front Fourier plane of the objective 4. A KLM-532-2000 laser with spatial coherence suppression is used as a radiation source. The structure of the probing light fields that implement 4D tomographic diagnostics is formed by a pair configuration of mirrors 5 and 5', 6 and 6', 7 and 7', forming beams oriented relative to the optical axis of the shadow device at angles $\theta_p = \pi(p-1)/4$, where the projection number is p = 1, …, 4. Overall dimensions of the mirrors are 100×15×145 mm. The Fourier spectrum of phase perturbations induced in probing fields by the object of study is localized in the frequency plane of objective 8, where a quadrant phase Hilbert filter 9 is placed [1]. The lens 10 of the high-speed video camera converts the filtered field, depending on the spectral characteristics of the light source, into analytical or Hilbert-coupled optical signals, which are recorded on the CCD matrix 11. The choice of the tomograph technical solution is due to the possibility of using a large field of view (400 mm) of the IAB-463M shadow device.

The use of a linear light source oriented along one of the spatial-frequency axes in combination with a quadrant phase Hilbert filter provides a one-dimensional Hilbert transform of the optical field p-tomographic component:

$$I_p(y_p, z) = \left| \frac{1}{\pi} \int_{-\infty}^{+\infty} \frac{s_p(y', z)}{y_p - y'} dy' \right|^2 = \left| \hat{s}_p(y_p, z) \right|^2,$$

where $I_p\left(y_p, z\right)$ is the signal intensity recorded by the video camera, $\hat{s}_p(y_p, z)$ is the signal Hilbert image $s_p\left(y_p, z\right) = e^{i\varphi_p(y_p, z)}$, $\varphi_p(y_p, z)$ is the phase function, which is determined by the Radon transform of the refractive index $n\left(x_p, y_p, z\right)$ in the local structure of the medium under study:

$$\varphi_p(y_p, z) = \frac{2\pi}{\lambda} \int_{x'}^{x''} \left[n(x_p, y_p, z) - n_\infty \right] dx_p,$$

λ – the wavelength, n_∞ is the air refractive index, x' and x'' are the entry and exit points of the beam relative to the local structure of the medium under study for a certain tomographic component.

An experiments series to study combustion processes was carried out on a Hilbert tomographic complex (figure 2).

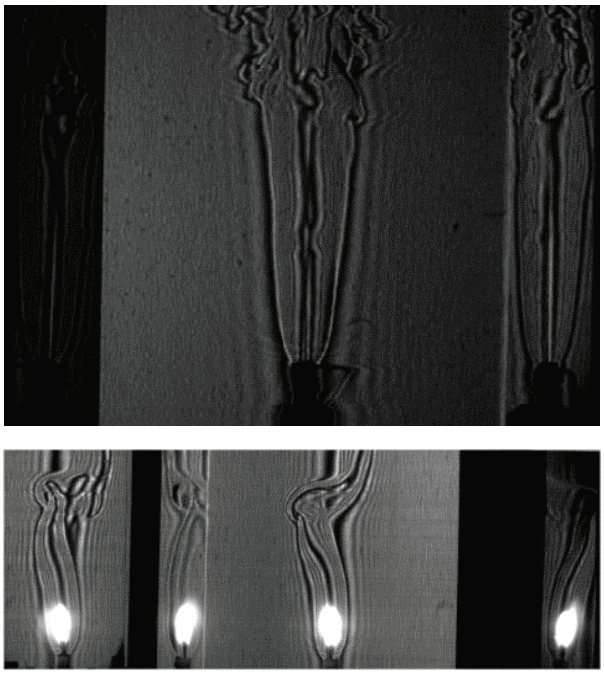

Figure 2: (*a*) 3R burner flame hilbertograms: projection $\theta_p = 3\pi/4$, front projection $\theta_p = 0$ and angle projection $\theta_p = \pi/4$ are shown in succession; (*b*) 4R candle flame hilbertograms: projection $\theta_p = \pi/2$, $\theta_p = 3\pi/4$, front projection $\theta_p = 0$ and angle projection $\theta_p = \pi/4$

3. The Gershberg-Papoulis method

The tomography inverse problem in a parallel setting is to restore the refractive index function $n = n(x, y)$ from the integrals values of it along the straight lines $L: \vec{r} \cdot \overrightarrow{e_\theta} = s$, $\vec{r} = (x, y)$ and $\overrightarrow{e_\theta} = (\cos\theta, \sin\theta)$:

$$\mathcal{R}_\theta n(s) = \int_L n(x, y)dl = \iint_{R^2} \delta(s - \vec{r} \cdot \overrightarrow{e_\theta}) n(x, y)dxdy.$$

Many inversion formulas for the Radon problem are based on the central section theorem [10], which states that the (one-dimensional) Fourier transform of the projection $\mathcal{R}_\theta n(s)$ is equal to the cross section of the two-dimensional Fourier transform of the function $n = n(x, y)$:

$$\widehat{\mathcal{R}_\theta n}(\omega) = F[n](W_\theta), \quad W_\theta = (\omega\cos\theta, \omega sin\theta).$$

This theorem underlies many algorithms of computed tomography, in particular, the back projection method [8].

The Gershberg-Papoulis algorithm is one of the most efficient methods for reconstructing functions from their Radon projections, especially in cases where the scanning directions number is small or their angular range is limited. The method essence lies in the fact that a priori information about the desired function $n(x, y)$ and its known projections $\mathcal{R}_\theta n(s)$ is used to create an initial approximation and subsequent correction in the coordinate and frequency spaces. The non-negativity and finiteness of the desired function are used as a priori information:

$$n(x, y) \geq 0;\ n(x, y) = 0;\ x^2 + y^2 \geq 1.$$

The C_M operator, acting in the spatial plane, defines these properties.

The function values $N(W) = F[n](W)$ in the directions along the vectors $\overrightarrow{e_p} = (\cos\theta_p, \sin\theta_p)$ are known in the Fourier plane from the Radon data. Thus, the Fourier transform of the desired function $n(x, y)$ is known on the set M:

$$M = \{W = \omega\overrightarrow{e_p}, -\infty < \omega < \infty\}.$$

If H_M is the characteristic function of the set M:

$$H_M = \begin{cases} 1, & W \in M \\ 0, & W \notin M \end{cases};$$

then the values are known

$$S_M(W) = H_M(W)N(W).$$

The following operations must be performed to reconstruct the refractive index function:

1. One-dimensional Fourier transforms are computed from known Radon data. Thus, the function S_M is determined, equal to the values of the two-dimensional Fourier transform of the desired function in the directions corresponding to the projections angles, and equal to zero at Fourier plane other points.
2. The initial approximation n^0 is determined: the inverse two-dimensional Fourier transform of the S_M function is performed. A priori information about the refractive index positiveness n and the area boundedness of its assignment is introduced (the C_M operator is applied).
3. A two-dimensional Fourier transform is performed from the initial approximation. The spectrum values in the directions corresponding to the projection angles are replaced by the values calculated in step 1.
4. The inverse two-dimensional Fourier transform of the function obtained at the previous step is performed and the C_M operator is applied to the result.
5. The criterion for the iterative process end is checked (if it is not fulfilled, then steps 3, 4 are repeated): the norm smallness of obtained tomogram deviation from its estimate at the previous stage Δ_m:

$$\Delta_m^2 = \frac{\sum_i \sum_j \left(n_{i,j}^m - n_{i,j}^{m+1}\right)^2}{\sum_i \sum_j \left(n_{i,j}^m\right)^2}.$$

As a result, the reconstruction algorithm can be represented as:

$$N^0 = S_M, \quad n^0 = C_M F^{-1}[N^0],$$
$$N^{m+1} = S_M + F^{+1}[n^m](1 - H_M), \quad n^{m+1} = C_M F^{-1}[N^{m+1}].$$

The use of the Gershberg-Papulis method for the refractive index reconstruction from hilbertograms is due to the following. The projection values for all selected observation angles are determined at those points that correspond to the Radon integrals along the straight lines passing through the nodes of the sampling grid when obtaining a digital image using a system of mirrors. The sampling grid nodes correspond to the photomatrix resolution. Therefore, the discrete analog of the central section theorem allows one to obtain initial data in the Fourier plane without preliminary interpolation.

4. Test objects reconstruction

Linear combinations of the following functions were considered to evaluate the application effectiveness of the Hershberg-Papulis method in recovering an unknown function from its Radon data obtained from four projections:

$$f(x,y) = A\, e^{1/a^2} e^{-1/\left|a - |\vec{r} - \vec{r}_0|\right|^2}\, Heaviside(a - |\vec{r} - \vec{r}_0|),$$
$$g(x,y) = A\, e^{-|\vec{r} - \vec{r}_0|^2/s^2},$$
$$h(x,y) = A\, Heaviside(a - |\vec{r} - \vec{r}_0|),$$

where

$$\vec{r} = (x,y), \qquad r = \sqrt{x^2 + y^2},$$
$$\vec{r}_0 = (x_0, y_0), \qquad r_0 = \sqrt{x_0^2 + y_0^2}.$$

The reconstruction results are shown in figures 3–9, where (*a*) is the original function, (*b*) is the reconstructed function by the Hershberg-Papulis method with indication of the root-mean-square recovery error Δ_m, (*c*) is the reconstructed function by the back projection method with filtering, (*d*) is the reconstructed function by the method of back projections without filtering.

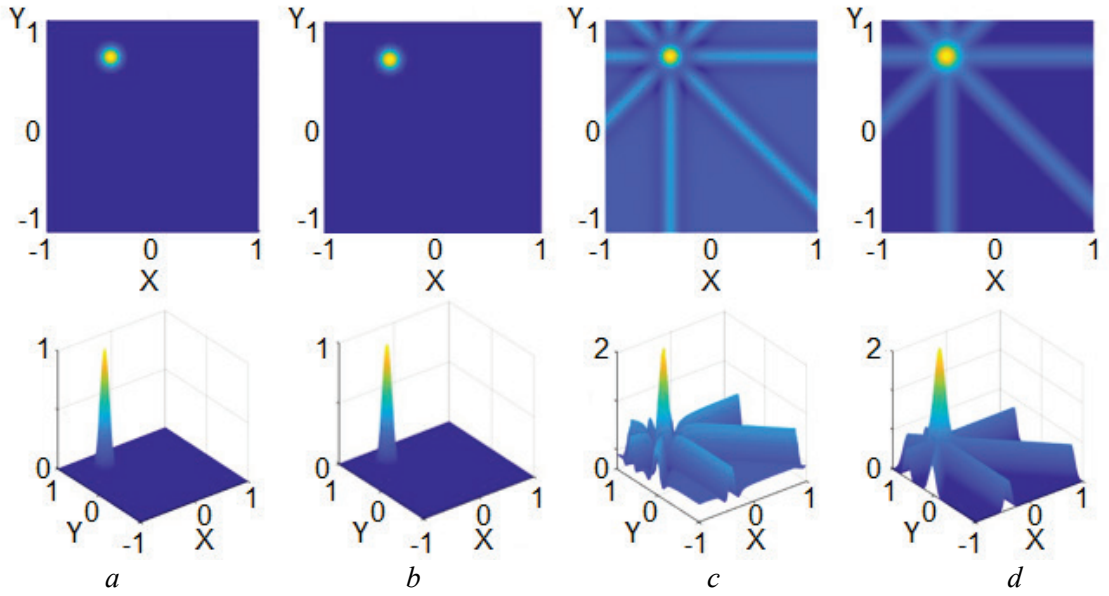

Figure 3: $n(x,y) = f_p(x,y)$; $x_0 = -0{,}4$; $y_0 = 0{,}65$; $A = 1$; $a = 0{,}3$;
$\Delta_m = 1{,}53\%$

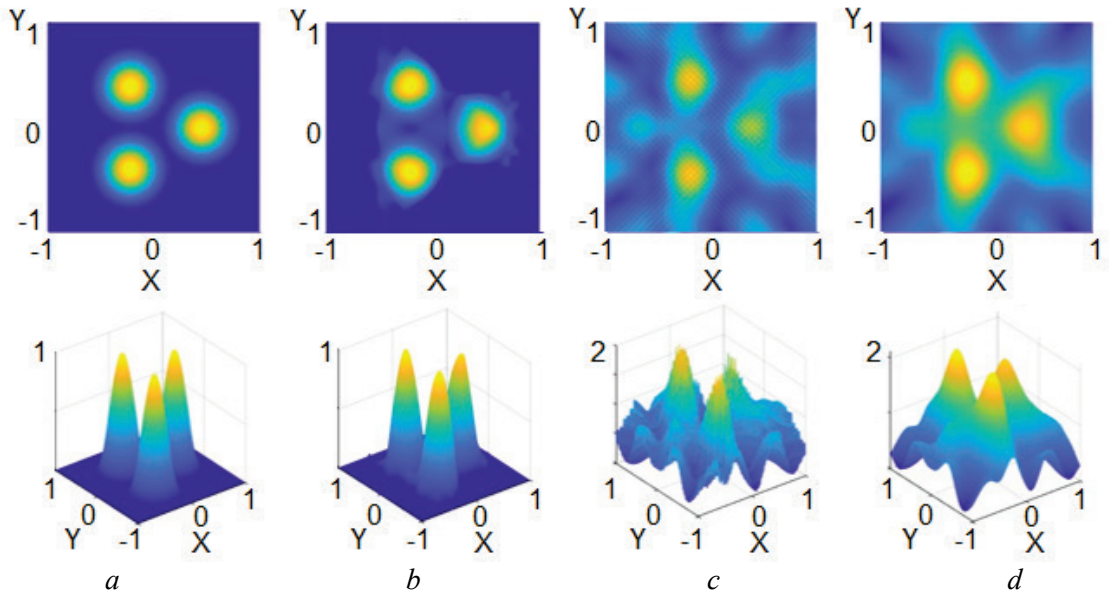

Figure 4: $n(x,y) = \sum_{p=1}^{3} f_p(x,y)$;
$x_0 = 0{,}45$ (1; –0,5; –0,5); $y_0 = 0{,}45$ (0; 0,86; –0,86);
$A = (1; 1; 1)$; $a = (0{,}5; 0{,}5; 0{,}5)$;
$\Delta_m = 11{,}53\%$

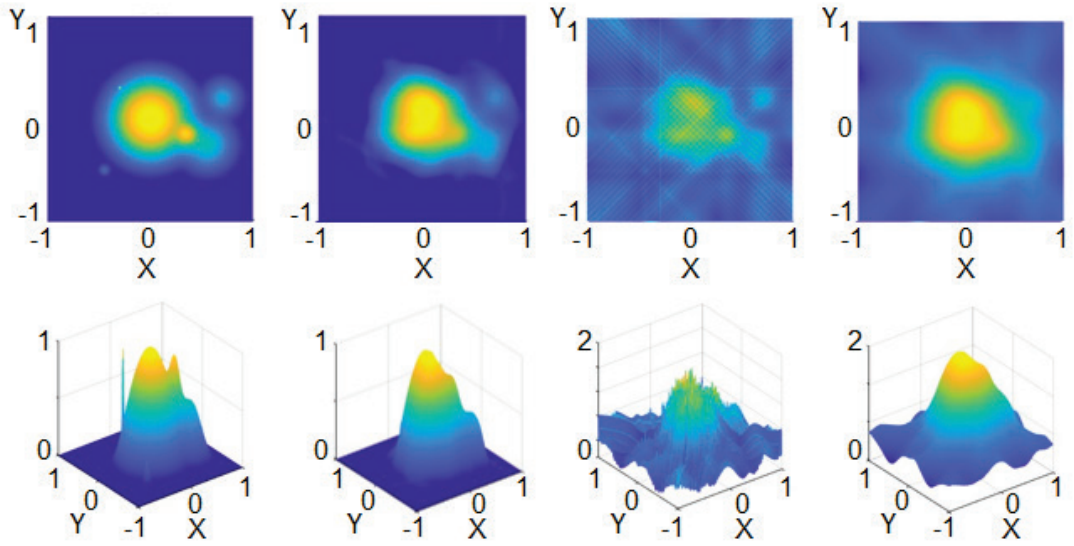

Figure 5: $n(x,y) = \sum_{p=1}^{6} f_p(x,y)$;
x_0 = (0; 0,35; 0,55; 0,7; –0,45; –0,3); y_0 = (0; –0,15; –0,25; 0,2; –0,5; 0,3);
A = (1; 0,3; 0,5; 0,4; 0,2; 0,8); a = (0,7; 0,3; 0,5; 0,4; 0,2; 0,1);
Δ_m = 9,99%

Further, functions similar to the test examples presented in [11] are considered.

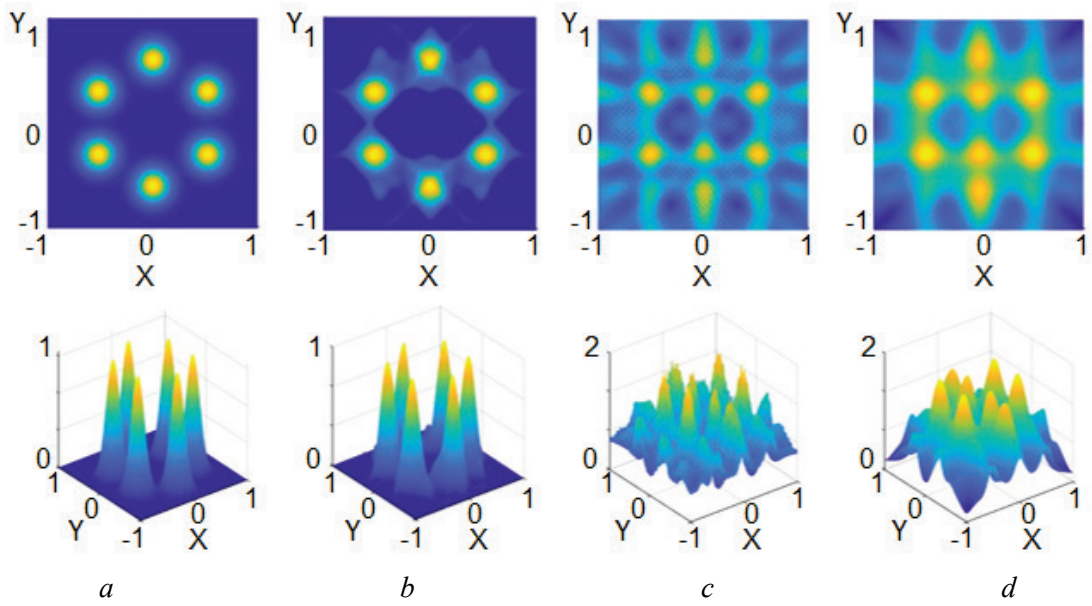

Figure 6: $n(x,y) = \sum_{k=1}^{6} g_k(x,y)$;
x_0 = 0,65 (0,86; 0; –0,86; –0,86; 0; 0,86); y_0 = 0,65 (0,5; 1; 0,5; –0,5; –1; –0,5);
A = (1; 1; 1; 1; 1; 1); s = (0,1; 0,1; 0,1; 0,1; 0,1; 0,1);
Δ_m = 18,44%

Since the Gershberg-Papoulis iterative method interpolates the reconstructed function spectrum by known values given on the straight lines corresponding to the scanning directions, the reconstruction result will be better if the original function Fourier spectrum is localized in the low spatial frequencies region. The given examples of model functions are an illustration of this provision.

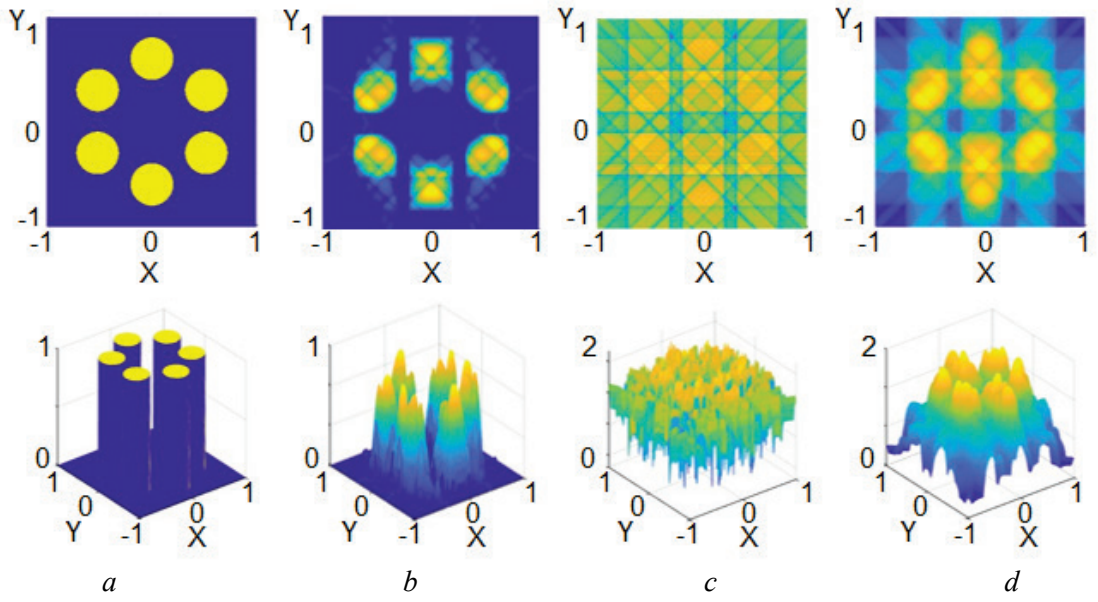

Figure 7: $n(x,y) = \sum_{p=1}^{6} h_p(x,y;a_p)$;
x_0 = 0,65 (0,86; 0; –0,86; –0,86; 0; 0,86); y_0 = 0,65 (0,5; 1; 0,5; –0,5; –1; –0,5);
A = (1; 1; 1; 1; 1; 1); a = (0,2; 0,2; 0,2; 0,2; 0,2; 0,2);
Δ_m = 34,85%

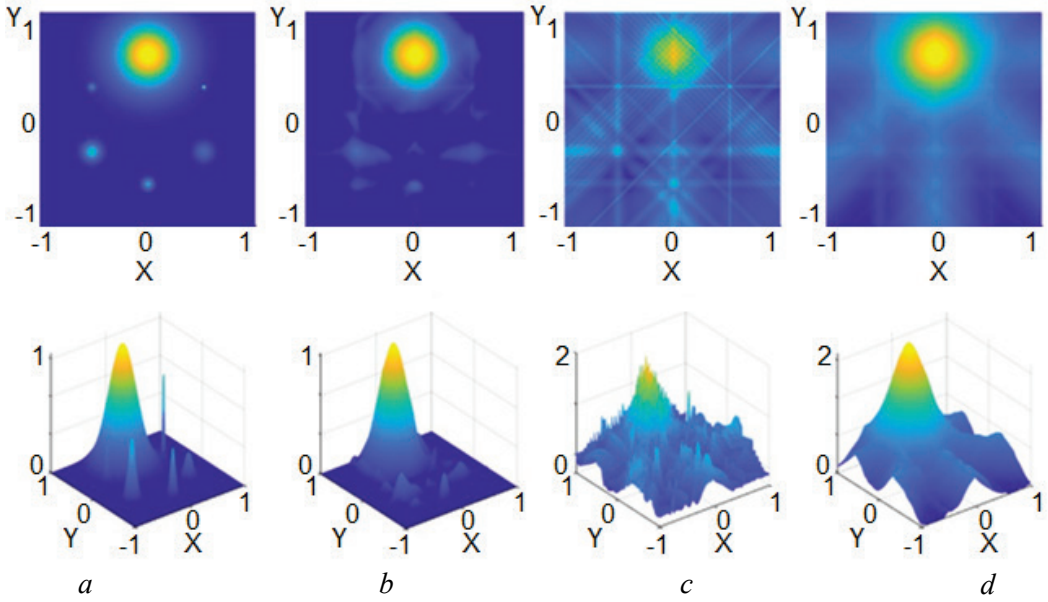

Figure 8: $n(x,y) = \sum_{p=1}^{6} g_p(x,y)$;
x_0 = 0,65 (0,86; 0; –0,86; –0,86; 0; 0,86); y_0 = 0,65 (0,5; 1; 0,5; –0,5; –1; –0,5);
A = (0,8; 1; 0,3; 0,5; 0,4; 0,2); s = (0,01; 0,2; 0,02; 0,05; 0,03; 0,05);
Δ_m = 10,92%

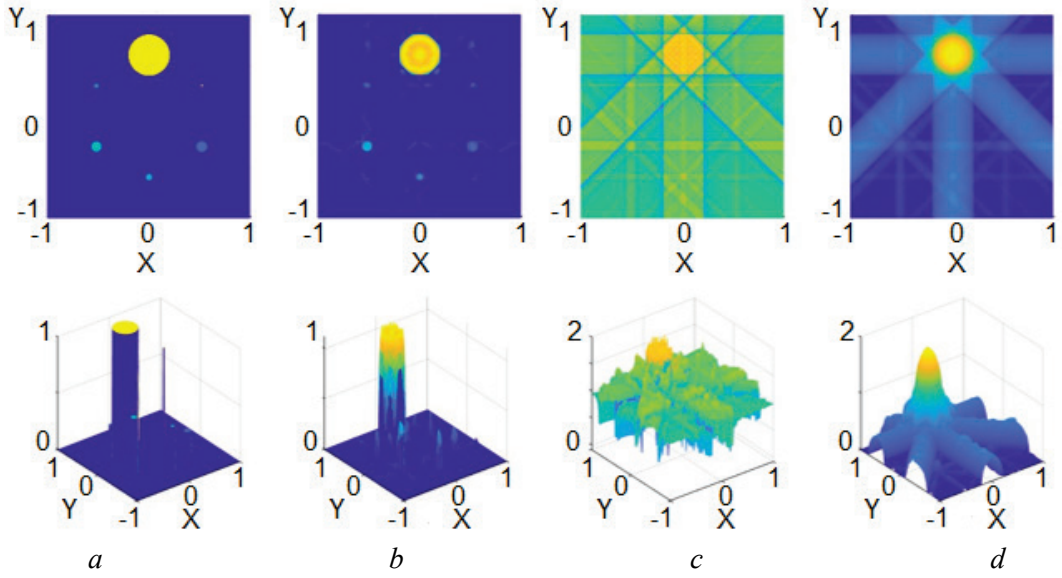

Figure 9: $n(x,y) = \sum_{p=1}^{6} h_p(x,y;a_p)$;
x_0 = 0,65 (0,86; 0; –0,86; –0,86; 0; 0,86); y_0 = 0,65 (0,5; 1; 0,5; –0,5; –1; –0,5);
A = (0,8; 1; 0,3; 0,5; 0,4; 0,2); a = (0,01; 0,2; 0,02; 0,05; 0,03; 0,05);
Δ_m = 14,66%

5. Conclusion

The possibility of using the Gershberg-Papulis method for solving the low-angle optical Hilbert diagnostics problem is investigated in this work. Numerical simulation was performed to evaluate the method effectiveness.

The Hershberg-Papoulis method is an important tool in the field of computed tomography and optics. It solves the problems associated with the images restoration with limited projections, and finds application in various fields of science and industry. However, it may be necessary to modify this method or use additional methods for more accurate image restoration.

6. Acknowledgements

The work of the first author was carried out within the framework of the state assignment of IM SB RAS (No. FWNF-2022-0009), and the work of the other authors was carried out within the framework of the state assignment of IT SB RAS (No. 121031800217-8).

7. References

[1] V. A. Arbuzov, Yu. N. Dubnishchev, Metody gil'bert-optiki v izmeritel'nykh tekhnologiyakh [Hilbert-optics methods in measurement technologies], NSTU University Publ., Novosibirsk, 2007.

[2] Yu. N. Dubnishchev, V. A. Arbuzov, E. V. Arbuzov, O. S. Zolotukhina, V. V. Lukashov, Polychromatic diagnostics of the flame with Hilbert verification of the visualized phase structure, Scientific Visualization 13 (2021) 1–8. doi:10.26583/sv.13.4.01.

[3] V. A. Arbuzov, E. V. Arbuzov, Yu. N. Dubnishchev, V. V. Lukashov, O. S. Zolotukhina, Optical diagnostics of hydrogen-air diffusion jet flame, Journal of Engineering Thermophysics 31 (2022) 402–413. doi:10.1134/S1810232822030031.

[4] G. G. Levin, G. N. Vishnyakov, Opticheskaya tomografiya [Optical tomography], Radio and Communications Publ., Moscow, 1989.

[5] Xiong Wan, Yiqing Gao, Qing Wang, Shuping Le, Shenglin Yu, Limited-angle optical computed tomography algorithms, Optical Engineering 42 (2003) 2659–2669. doi:10.1117/1.1595104.
[6] R. W. Gerchberg, Super-resolution through error energy reduction, Opt. Acta. 21 (1974) 709–720. doi:10.1080/713818946.
[7] A. A. Papoulis, New algorithm in spectral analysis and band-limited extrapolation, IEEE Transactions on Circuits and Systems 22 (1975) 735–742. doi:10.1109/TCS.1975.1084118.
[8] V. V. Pikalov, T. S. Melnikova, Nizkotemperaturnaya plazma. Tomografiya plazmy (tom 13) [Low temperature plasma. Plasma tomography (volume 13)], Nauka Publ., Novosibirsk, 1995.
[9] A. F. Belozerov, Opticheskiye metody vizualizatsii gazovykh potokov [Optical methods for visualization of gas flows], Kazan Technical University Publ., Kazan, 2007.
[10] A. S. Kravchuk, Osnovy komp'yuternoy tomografii: Posobiye dlya studentov [Fundamentals of Computed Tomography: Student's Guide], Moscow, 1999.
[11] V. V. Pickalov, D. I. Kazantsev, New iterative reconstruction methods for fan-beam tomography, Inverse Problems in Science and Engineering 26 (2018) 773–791. doi:10.1080/17415977.2017.1340946.